Bollettino di Geofisica Teorica ed Applicata Vol. 52, n. 3, pp. 367-387; September 2011
DOI 10.4430/bgta0019

# The 2009 L'Aquila (central Italy) seismic sequence

L. Chiaraluce[1], C. Chiarabba[1], P. De Gori[1], R. Di Stefano[1], L. Improta[1], D. Piccinini[1], A. Schlagenhauf[2], P. Traversa[2], L. Valoroso[1] and C. Voisin[2]

[1] *Istituto Nazionale di Geofisica e Vulcanologia, Rome, Italy*
[2] *Laboratoire de Géophysique Interne et Tectonophysique, Grenoble, France*

(Received: April 7, 2010; accepted: October 15, 2010)

***ABSTRACT*** On April 6 (01:32 UTC) 2009 a $M_W$ 6.1 normal faulting earthquake struck the axial area of the Abruzzo region in central Italy. The earthquake heavily damaged the city of L'Aquila and its surroundings, causing 308 casualties, 70,000 evacuees and incalculable losses to the cultural heritage. We present the geometry of the fault system composed of two main normal fault planes, reconstructed by means of seismicity distribution: almost 3000 events with $M_L \geq 1.9$ occurred in the area during 2009. The events have been located with a 1D velocity model we computed for the area by using data of the seismic sequence. The mainshock, located at around a 9.3 km depth beneath the town of L'Aquila, activated a 50° (+/- 3) SW-dipping and ~135° NW-trending normal fault with a length of about 16 km. The aftershocks activated the whole 10 km of the upper crust up to the surface. The geometry of the fault is coherent with the mapped San Demetrio-Paganica and Mt. Stabiata normal faults. The whole normal fault system that reached about 40 km of length by the end of December in the NW-trending direction, was activated within the first few days of the sequence when most of the energetic events occurred. The main shock fault plane was activated by a foreshock sequence that culminated with a $M_W$ 4.0 on March 30 (13:38 UTC), showing extensional kinematics with a minor left lateral component. The second major structure, located to the north close to Campotosto village, is controlled by an $M_W$ 5.0 event, which occurred on the same day of the main shock (April 6 at 23:15 UTC), and by an $M_W$ 5.2 event (April 9 at 00:53 UTC). The fault plane shows a shallower dip angle with respect to the main fault plane, of about 35° with a tendency to flattening towards the deepest portion. Due to the lack of seismicity above a 5 km depth, the connection between this structure and the mapped Monti della Laga fault is not straightforward. This northern segment is recognisable for about 12-14 km of length, always NW-trending and forming a right lateral step with the main fault plane. The result is a *en-echelon* system overlapping for about 6 km. The seismicity pattern also highlights the activation of numerous minor normal fault segments within the whole fault system. The deepest is located at around a 13-15 km depth, south of the L'Aquila mainshock, and it seems to be antithetic to the main fault plane.

**Key words:** L'Aquila earthquake, fault system, central Italy.

## 1. Introduction: the seismotectonic context

During the Quaternary, the region of the central Apennines hit by the 2009 $M_W$ 6.1 L'Aquila event

 

(Fig. 1), was deformed by active extensional tectonics following the eastward migration of the Apenninic compressional front. The result is a broad and complex system of normal faults developed in areas previously affected by compression [Galadini and Galli (2000) and references therein].

In this portion of the chain, extension occurs on an 50 km wide area (Selvaggi *et al*., 1997) that is accommodated, at least, on two major sub-parallel NW-SE trending normal fault systems (Vezzani and Ghisetti, 1998; Barchi *et al*., 2000; Galadini and Galli, 2000; Roberts and Michetti, 2004), unlike the contiguous northern and southern Apennines. The activity of these two systems produced large intermountain extensional basins such as L'Aquila, Sulmona and Fucino basins, filled by Plio-Quaternary continental sediments (Cavinato and De Cellis, 1999; Galadini and Galli, 2000). During the Quaternary, the normal and normal-oblique faulting was synchronous to a regional uplift (e.g., D'Agostino *et al*., 2001; Galadini and Galli, 2003) and the NE-trending extension is considered continuously active at least since the Early Pleistocene. The current rate of extension is 2-3 mm/year (Hunstad *et al*., 2003) and its orientation is consistent with available focal mechanism solutions (Montone *et al*., 2004), borehole break-out (Mariucci *et al*., 1999) and geological data (Lavecchia *et al*., 1994). Field, geology-based studies revealed the location and geometry of major faults. Some of them are thought to be responsible for the larger historical earthquakes that occurred in the region, such as the Fucino fault system associated to the 1915 $M_S$ 7.0 earthquake [Fig. 1; e.g., Ward and Valensise, (1989)].

The closest and largest damaging historical earthquakes that struck the region occurred in 1461 close to the city of L'Aquila ($I_{max}$=X), and in 1703 slightly to the north [$I_{max}$=XI; CPTI Working Group (1999)]. The location and geometry of the seismogenic sources of these events are not yet constrained, so we decided to show both the macro-seismic epicentre and the locations (colour coded points) that for each event recorded the largest intensity in Fig. 1. Some authors [e.g., Atzori *et al*. (2009), among others] suggest that the 1461 event may have occurred on the Paganica-San Demetrio segment [SDP; mapped by Bagnaia *et al*. (1992)] responsible for the 2009 mainshock. However, despite dense temporary seismic surveys carried out in the area, the geometry, at depth, of the larger faults mapped as active is still unconstrained (Bagh *et al.,* 2007) because background seismicity in the inter-seismic period appears sparsely distributed without putting in evidence clear fault planes (Chiaraluce *et al*., 2009).

In Fig. 1, we also report the larger instrumental seismic sequences that occurred in the region together with the location and focal mechanisms of the main events. From NW to SE, the Colfiorito (Chiaraluce *et al*., 2003) and Norcia (Deschamps *et al*., 1984) sequences occurred in 1997 and 1979, respectively. Both sequences activated SW-dipping normal faults. South-eastwards, we report the seismicity of the 2009 L'Aquila sequence with its main shock location and dip-slip focal mechanism solution (Scognamiglio *et al*., 2010).

During the past 20 years the area has only been affected by minor seismic episodes (in 1992, 1994 and 1996) and minor sequences are located close to the L'Aquila area, with a maximum magnitude $M_L$=4.0 (De Luca *et al*., 2000; Pace *et al*., 2002; Boncio *et al*., 2004; Ciaccio *et al*., 2009).

In this study, we present a seismicity pattern for the whole of 2009 in the source region of the L'Aquila earthquake. We use hypocentral locations obtained by using a 1D gradient P-wave velocity model and $V_P/V_S$ ratios, computed for the area, to show the first order geometry of the activated normal fault system. The earthquakes have been recorded by the permanent Stations of

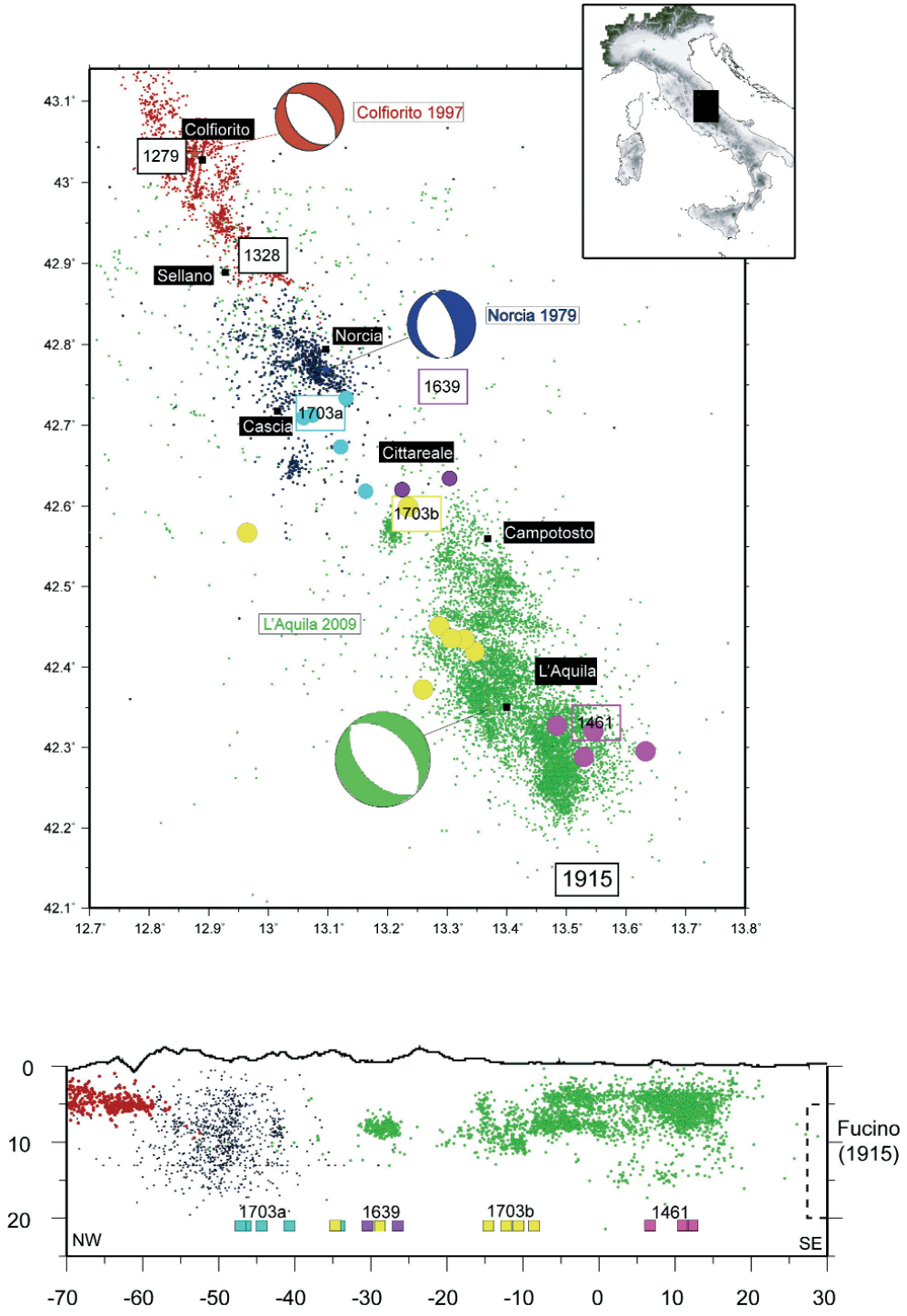


Fig. 1 - Map view (a) and longitudinal cross section (b) of the historical (Working Group CPTI, 1999) and instrumental seismicity plus focal mechanisms of the largest events [Chiaraluce *et al*. (2007) and reference therein and Scognamiglio *et al*. (2010)]. Large circles (in map) represent the location of the largest intensities for each historical event. As a reference, these points have been reported also in the cross section at a arbitrary depth of 20 km to do not overlap with instrumental seismicity (see text for details). Whilst the boxes containing dates are the macro-seismic epicentres of the corresponding historical earthquakes.

the National Seismic Network (RSNC) managed by the Istituto Nazionale di Geofisica e Vulcanologia (INGV) to April 6, and then by stations of the INGV temporary network, available a few hours after the L'Aquila mainshock. For two months after April, we also benefited from data from an additional temporary network installed by the Laboratoire de Géophysique Interne et Tectonophysique (LGIT) of Grenoble. We use seismicity distribution and focal mechanisms of the major events to describe the geometry and kinematics of the activated fault system.

## 2. Earthquake location and seismic catalogue

### *2.1. Velocity model and $V_P/V_S$*

In Fig. 2A, we show the two P-wave 1D velocity models available for the area together with the gradient velocity model we used. The model by Bagh *et al*. (2007; black line in Fig. 2A) was computed with the Genetic Algorithms technique for a larger area including the study region. The model by Chiarabba *et al*. (2009; grey line in Fig. 2A) was computed with preliminary data of the L'Aquila sequence by inverting P- and S-wave arrival times with the VELEST code (Kissling *et al*., 1994). Both those velocity models are prone to the introduction of artefacts, namely horizontal earthquake alignments along discontinuities, due to the use of a layer-cake model. Such artefacts are more likely to be present when trying to represent a 3D complex structure with a 1D velocity model, while they disappear in 3D earthquake locations (Di Stefano *et al*., 2011). To choose the best reference 1D velocity model for our data set we performed several preliminary earthquake location tests, trying to avoid artificial alignments of seismicity. Based on our results we ended up with the idea that a 1D layered cake model is in this case not adequate to be used for accurate 1D earthquake locations due the very complex 3D structure of the L'Aquila region. Thus, we prefer to use a smooth-gradient model (red line in Fig. 2A) showing P-wave velocity values very close to those of models A and B, but continuously defined top to bottom. Lower P-wave velocities at the surface, with respect to the other two models, are compatible with the presence of lower velocity sedimentary units outcropping in the epicentral area and in the northern sector of the fault system (Campotosto area). The gradient velocity model used in this study consists of a $V_P$ velocity that increases linearly from $V_0$ (5.0 km/s) at the surface by 0.15 km/s per kilometre until the half space is reached at a depth of 10 km. The velocity within the half space is 6.51 km/s.

The mean $V_P/V_S$ ratio was determined by using a cumulative Wadati diagram. Di Luccio *et al*. (2010) and Lucente *et al.* (2010) observed that the ratio changed with time during the sequence and mainly before and after the mainshock occurrence. In agreement with these studies, we recovered one value for the foreshocks (1.86) and a different one for the aftershocks (1.90). The Wadati diagrams in Fig. 2B and 2C illustrate the robustness of these measurements.

### *2.2. Parameters setting and data weighting in the location procedure*

A few hours after the main shock occurrence, numerous temporary stations were installed both in the epicentral area and at the edge of the fault system, with a double aim: to reduce the average spacing from stations from about 25 km (of INGV permanent network) to ~8 km and to be able to follow the spatio-temporal seismicity pattern. This emergency intervention allowed us to obtain very high quality locations throughout the seismic sequence evolution. We compute earthquake locations with the Hypoellipse code (Lahr, 1989) setting parameters differently for

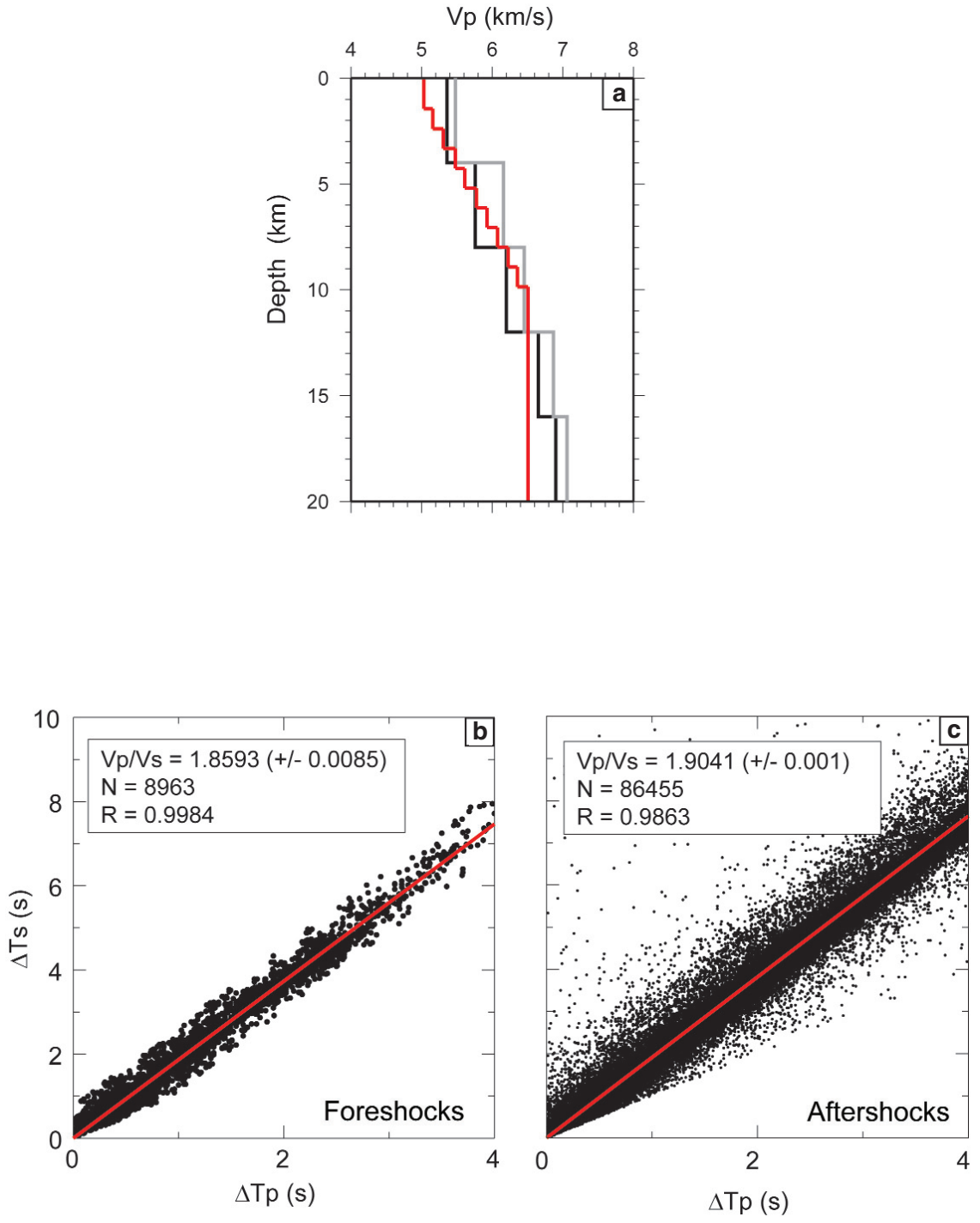


Fig. 2 - One-dimensional P-wave velocity models (a): black line for Bagh *et al*. (2007), grey line for Chiarabba *et al*. (2009) and red line for the gradient model used in this study. Wadati diagram of the $V_P/V_S$ ratio respectively for the foreshock (b) and aftershock sequence (c).

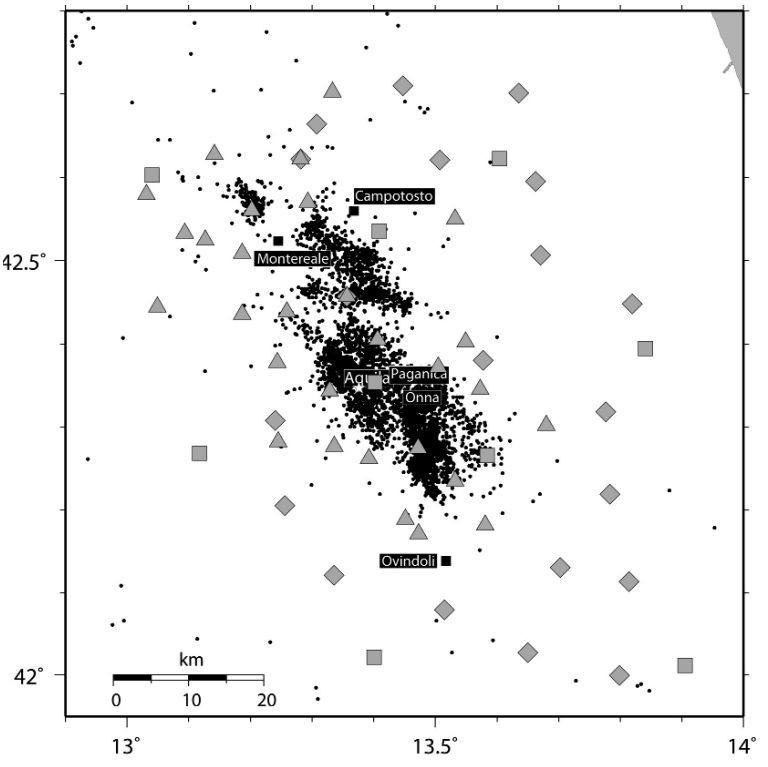


Fig. 3 - Seismic station distribution: grey squares indicate the RSNC stations, while triangles and diamonds show the location of the INGV and LGIT mobile networks, respectively.

different time intervals modulated on the network geometry evolution. Luckily, this prompt expansion and improvement of the network density and geometry, allowed us to follow the expansion of the epicentral area due to the activation of secondary structures after the mainshock occurrence. We divided the whole period into 5 different time windows in reason of the mean distance between the available seismic stations (see Table 1): 1) the stations of the RSNC (grey squares in Fig. 3), with mean distance of 25-30 km (from January 1 to the 12:00 p.m. of April 6); 2) RSNC plus the first 8 stations of the INGV mobile network installed a couple of hours after the mainshock occurrence (from the 12:00 p.m. of April 6 to April 7), with mean distance of 20 km; 3) RSNC plus all of the 20 INGV mobile network stations (grey triangles in Fig. 3) installed with a maximum distance of about 15 km (from April 7 to 9); all the local and permanent INGV stations plus other 20 stations of the

Table 1 - Networks available in 2009 for the Abruzzo region. See the text for the details of the installation timing of the temporary stations during the first hours-days after the main shock occurrence. PN: permanent network; MN: mobile network.

| J | F | M | A | M | J | J | A | S | O | N | D | Month |
|---|---|---|---|---|---|---|---|---|---|---|---|---|
| x | x | x | x | x | x | X | x | x | x | x | X | RSNC-PN |
| | | | x | x | x | X | x | x | x | x | X | INGV-MN |
| | | | x | x | x | | | | | | | LGIT-MN |

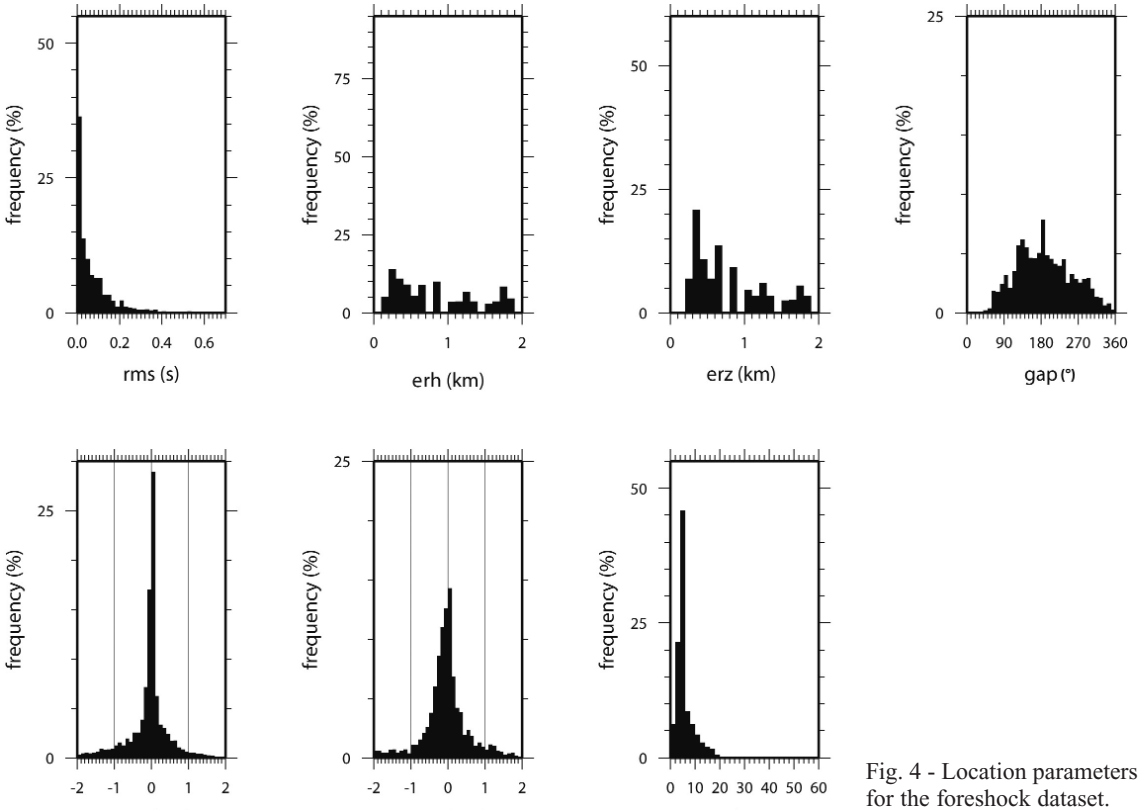


Fig. 4 - Location parameters for the foreshock dataset.

LGIT mobile network (grey diamonds in Fig. 4) that further reduced the spacing below 10 km (from April 9 to June 26); 5) the last period, going from the end of June to the end of 2009, has the same configuration as the third one. In the location procedure, we changed the weighting scheme with distance and the azimuthal coverage, according to the network evolution. We also used the elevation correction option using the first layer velocity up to a mean topography of 500 m that we derived computing the mean altitude of the station position.

### *2.3. Foreshock and aftershock catalogues*

We compiled the foreshock and aftershock catalogues by applying two different sets of selection parameters, based on the different network geometries illustrated above.

For the foreshocks that we define here as the events occurred in the study region from January 1 to April 6 at 1:30 a.m. UTC, only data recorded at stations of the RSNC are available. Due to the lower number of available stations, we decided to reprocess the data directly from the continuous recordings of all the stations located within 100 km from the mainshock, by using a more sensible triggering algorithm with the aim of detecting a larger number of smaller magnitude earthquakes. The triggering algorithm pinpointed 2861 coincidences at a minimum number of three stations. Then, we ran our automatic picking code on these data [MPX: Aldersons *et al*. (2009)] for P- and S-waves. We ended up with 1716 traceable events that after the first location process show the resolution parameters in Fig. 4. From these data, we selected

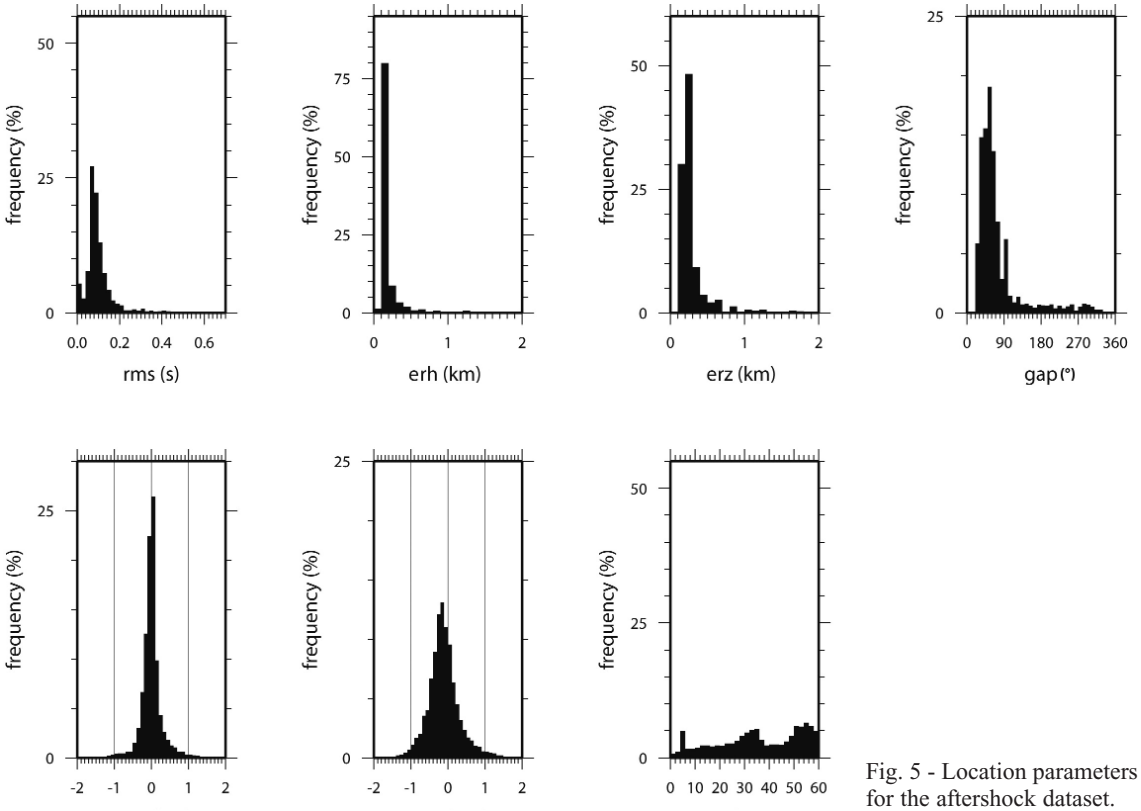


Fig. 5 - Location parameters for the aftershock dataset.

a final subset of ~600 well located events with a final rms < 0.4 s, azimuthal gap less than 200°, a minimum number of 4 arrival times and horizontal/vertical (ERH-Z) formal errors < 1.5 km.

For the aftershocks (from April 6 at 01:32 UTC to the end of 2009), we selected all the events with $M_L \geq 1.9$ from the whole catalogue of 18,867 events recorded and located within the epicentral area by personnel on duty at the INGV National Earthquake Centre 24 hours a day. No triggering algorithm was applied. We simply cut waveforms 50 s and 120 s before and after the origin time of the event respectively. Then, we ran the MPX on each earthquake. From the start we had 3044 events (location parameters are reported in Fig. 5), and we ended up with 2643 events with rms < 0.2 s, ERH-Z < 1 km, gap < 200° and more than 8 P- and 4 S-readings.

The very high quality of the absolute hypocentral locations for both data sets mainly derives from the exceptional performance of the automatic picker that has its main strength in the homogeneity of data weighting (Aldersons *et al*., 2009).

## 3. Seismicity pattern

In the spatio temporal evolution diagram (Fig. 6), we observe that the seismicity before and after the occurrence of the foreshock (March 30 at 13:38; $M_W$ 4.0) generally took place in the L'Aquila area. Soon after the mainshock (April 6 at 01:32 UTC; $M_W$ 6.1) seismicity started to

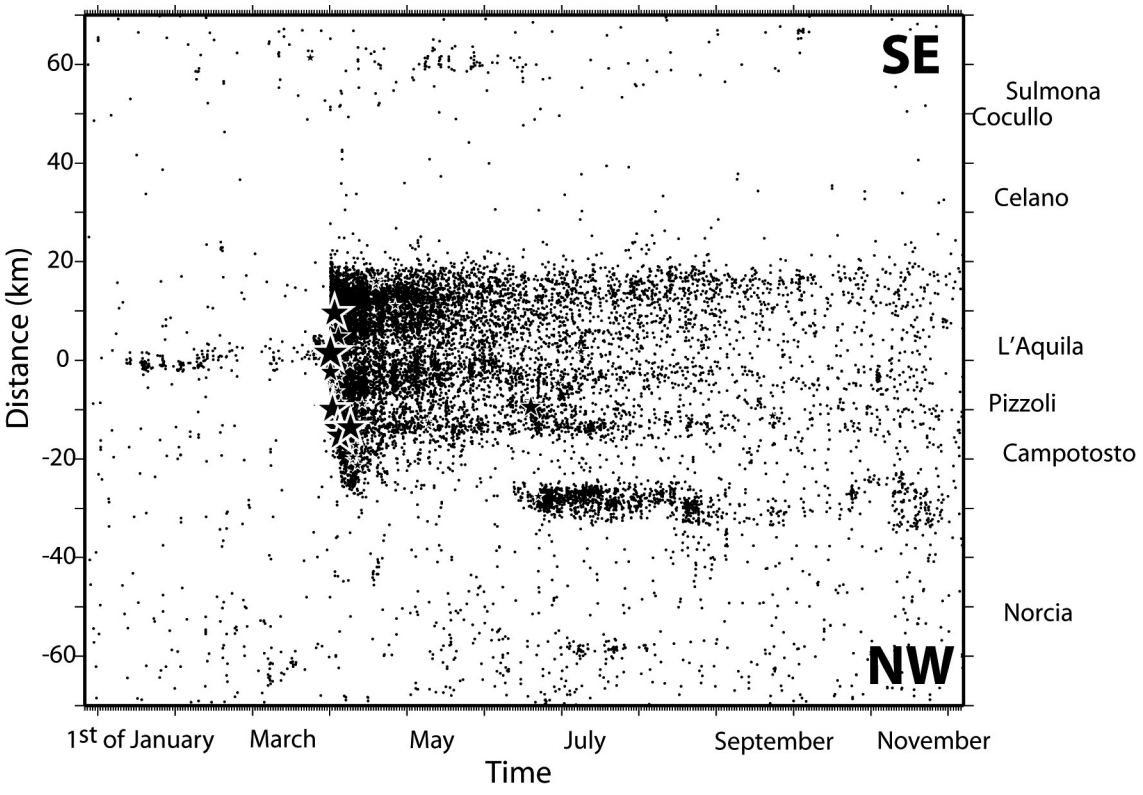


Fig. 6 - Spatio-temporal evolution of the seismicity in the epicentral area for the entire 2009.

spread migrating towards the Campotosto village, located to the NW. Here, the other main fault segment was activated within the first couple of days, as indicated by an $M_W$ 5.0 event that occurred on the same day of the main shock (April 6 at 23:15 UTC) and by an $M_W$ 5.2 event on April 9 (at 00:53 UTC). In general, the larger amount of energy was released within the first week of the aftershocks by events located on these two main fault planes. In the following three months, minor events mostly occurred within the whole main system, until the end of June when seismicity started to cluster around the Cittareale area located about 10 km to the north-westernmost part (Fig. 1). Though the larger event of this latter cluster is an $M_W$ 3.5 (June 25 at 21:00 UTC), the seismicity rate in this small area was high enough to be clearly visible on the curve showing the cumulative number of events for the whole period (Fig. 7). Also the activation of the flat and deepest portion of the Campotosto segment, occurred at the end of June with a main event of $M_W$ 4.4 (June 22 at 20:58 UTC; brown star in section 9 of Fig. 10) that contributed to this acceleration in the seismic release.

The majority of earthquakes in terms of cumulative number of events versus time, occurred in the week after the mainshock (black star in Fig. 7), and for the first three months after, we detected an Omori like decay: a rapid increase in the rate of production followed by an abrupt decay with time [inverse power, Omori (1895)].

The distribution of the seismicity versus depth (Fig. 8) shows that the majority of the events

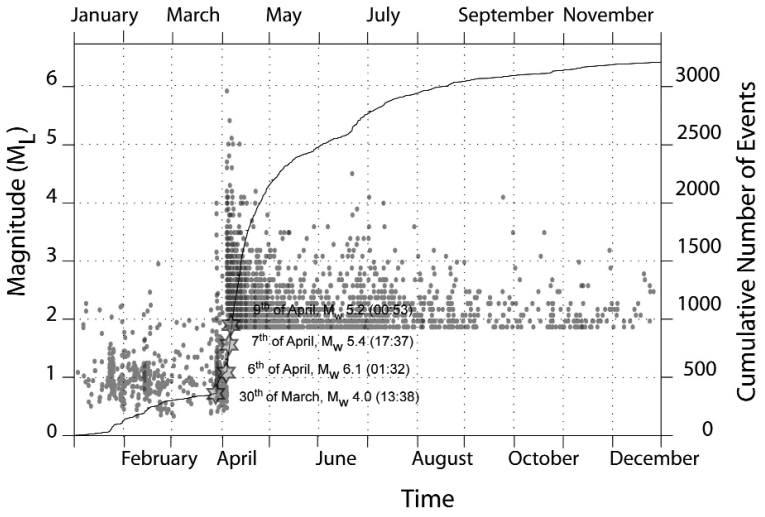


Fig. 7 - Cumulative number (black curve) and magnitude distribution of events (grey points), versus time.

occurred between 2 and 11 km of depth, but we also observed a deeper peak around 15 km. This depth interval of the seismogenic volume for this portion of the Abruzzo region, in agreement with Bagh *et al*. (2007), confirms that in this portion of the central Apennines the width of the active volume is at least 4 km thicker than in the northern Apennines. Fig. 8 also shows that the foreshocks (red line) do not generally occur at less than a depth of 6 km; however, the majority of large events (purple line) nucleate between 6 and 10 km of depth. Only one large event, with

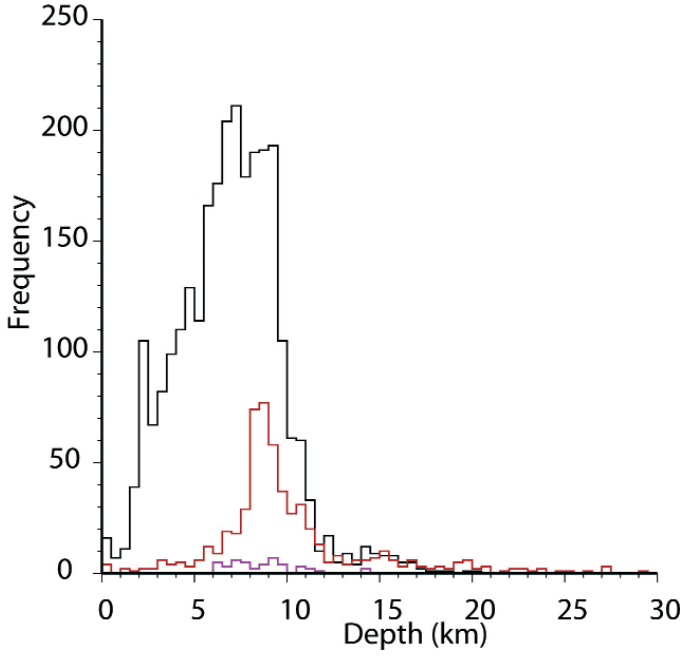


Fig. 8 - Number of events versus depth for the foreshocks (red line), aftershocks (black line) and events larger than $M_W$ 4.0 (purple).

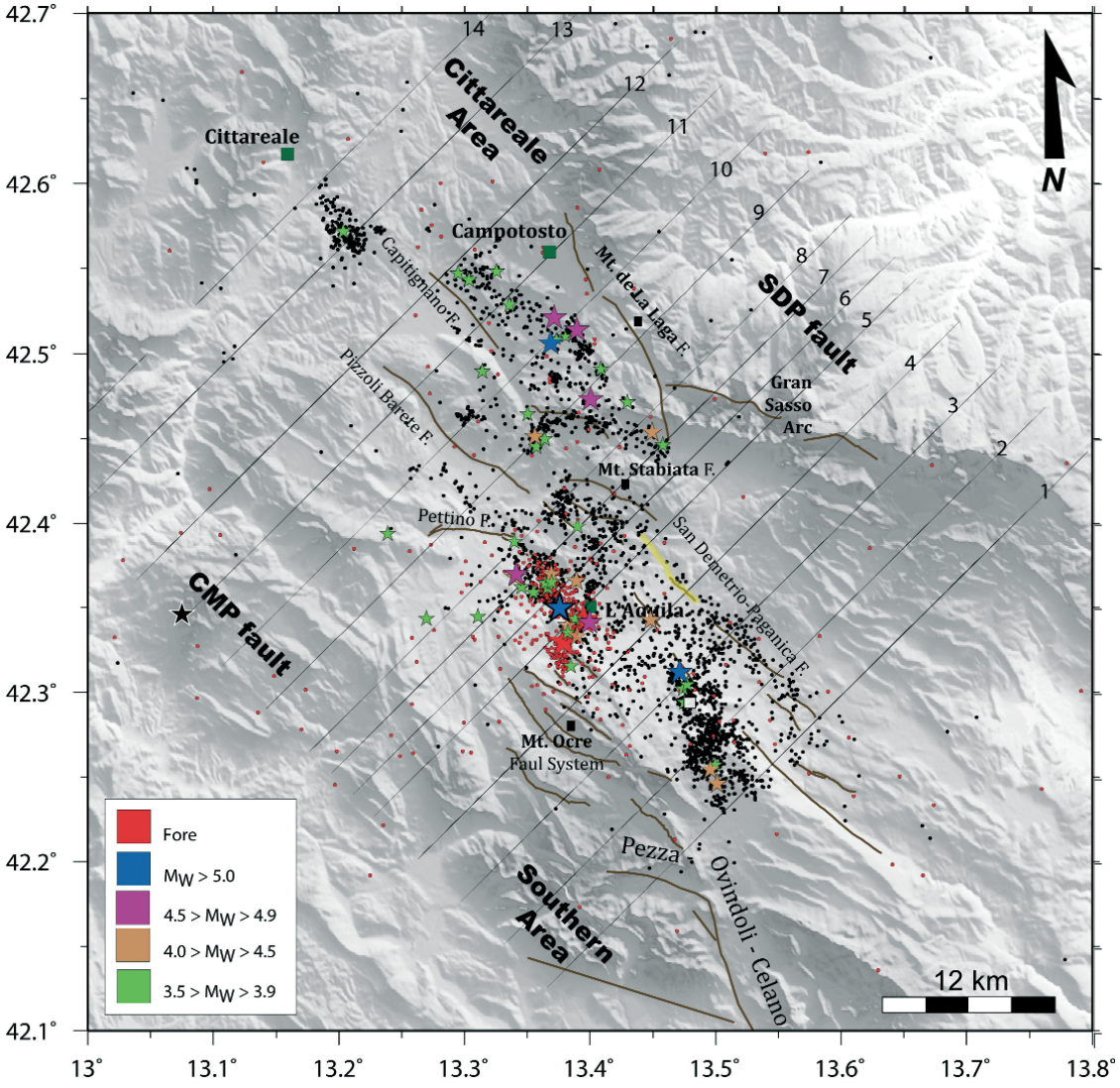


Fig. 9 - Map view of seismicity distribution: red points for foreshocks and black points for aftershocks. The locations (stars) of the larger events ($M_W$>3.5) of the sequence are reported colour coded by their size. Dark brown lines represent the Quaternary mapped normal faults [EMERGEO Working Group (2010) and reference therein]. The N45°E-trending thin lines are the traces of the 14 vertical cross sections of Fig. 10. In yellow we trace also the main surface breakages as mapped by the EMERGEO Working Group (2010).

$M_W$ 5.4 occurred around 14 km depth (April 7 at 17:47 UTC).

By the end of December, the maximum length of the fault system imaged by earthquake distribution is in the order of 40 km along the N45°W-trending direction (Fig. 6).

## 4. Fault system geometry

In this paragraph, we use seismicity distribution to reconstruct the geometry of the activated

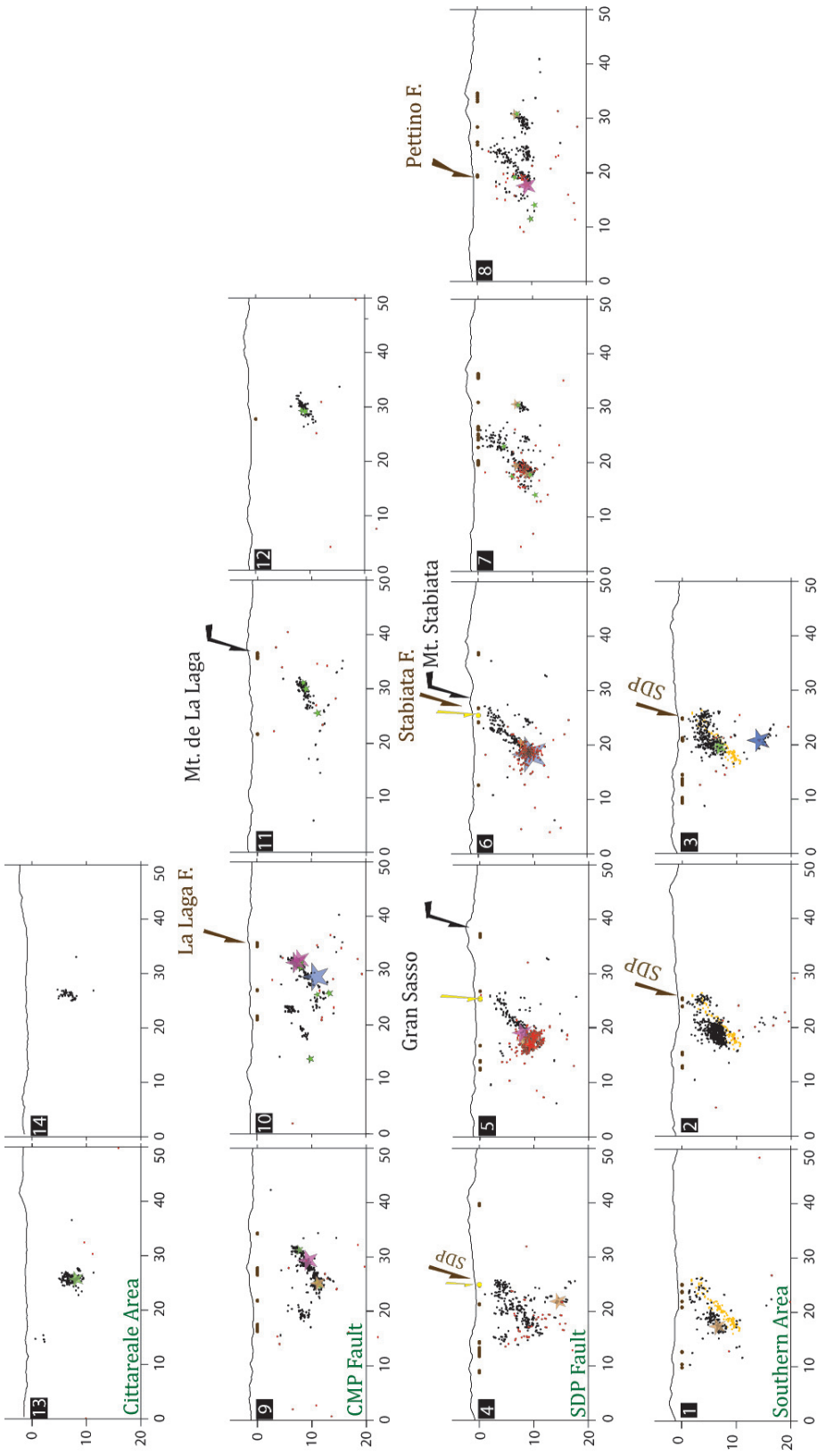


Fig. 10 - Vertical cross sections for the southern (a), L'Aquila (b), Campotosto (c) and Cittareale (d) areas. We report with the brown points located at 0 km of elevation the intersection between mapped fault and cross section traces. While yellow points indicate the intersections between the surface breakage and section traces. We report also the names of the most significative faults and geographic locations. Note that in the majority of the cross sections of Fig. 10a we project also the seismicity of cross section number 20 where it is easy to appreciate the SDP-MS fault geometry.

normal fault system. Hypocentral locations of the 561 foreshocks (red points) and 2643 aftershocks (black points) appear in the map view in Fig. 9 and in a set of vertical cross sections in Fig. 10. In the map view, we also report the mapped active faults of the area (brown lines in Fig. 9) and the ~5 km of surface breaks mapped by the EMERGEO Working Group (2010) the days soon after the mainshock occurrence (yellow line). The cross sections have been drawn perpendicular to the average strike of the main structures [N45°E; Anzidei *et al*. (2009) and Atzori *et al*. (2009)]. Section widths are symmetrical (NW-SE) perpendicularly to the trace but the width of each section is different to better describe the geometry of the specific portion. Seismicity in each cross section never overlaps. On the map and in the sections, stars depict all the events with $M_W$>3.5 (Scognamiglio *et al*., 2010), with dimension and colour code based on the magnitude.

### *4.1. The southern area*

This area is delimited to the north by the presence of the largest and deepest event of the sequence: an $M_W$ 5.4, that occurred on April 7 at 17:47 UTC at 14.1 km of depth (blue star in section 3 of Fig. 10; see location in map in Fig. 9). This event is characterised by a small number of aftershocks occurring in the first couple of days after. The focal mechanism (Fig. 11) shows a normal faulting solution with a minor strike slip component. Based on the distribution of the few aftershocks, we select the ENE-dipping plane at high angle (~60°) in between the two of the nodal planes for this event, denoting a left lateral component in the dip slip kinematics. This deep and small segment, less than 4 km long, is antithetic to the main SW-dipping L'Aquila fault plane.

The shallower seismicity shows some minor alignments but not a clear geometry of a main fault plane. To better understand the geometry and the role of these minor segments we superimposed the seismicity contained in one section that well image the main L'Aquila plane (yellow points) to the first three cross sections of Fig. 10. This portion of the system is missing a clear major plane but some events in section 3 seem to delineate few minor fault segments synthetic to the main system (sections 6, 11 and 12). Southwards (sections 1 and 2), we observe the presence of a main cluster showing no specific alignment. The main remark here is that all these structures are located in the main fault hanging-wall. The absence of the main fault plane south of section 3 is in agreement with the L'Aquila 2009 fault model proposed by Anzidei *et al*. (2009) obtained by modelling the horizontal and vertical coseismic surface displacements observed at a set of 5 GPS stations. We report, in Fig. 9, the location of the southernmost GPS station named CADO located about 16 km south of the mainshock along strike, whose coseismic displacement signs the end of the main fault plane. We acknowledge that this area needs to be investigated possibly with higher resolution locations.

### *4.2. L'Aquila area*

In this area, seismicity distribution clearly images the main fault plane of the system (sections 4 to 8 of Fig. 10): a 50° (+/- 3) SW-dipping plane striking at about N135°E, activated by the mainshock of April 6 at 01:32 UTC with $M_W$ 6.1 (blue star in section 6). The mainshock nucleated at an ~9.3 km depth at the base of the seismicity and shows a focal mechanism in perfect agreement with the geometry of the fault. The seismicity distribution clearly images the fault plane for a length of at least 16 km activating all the first 10 km of the upper crust up to the

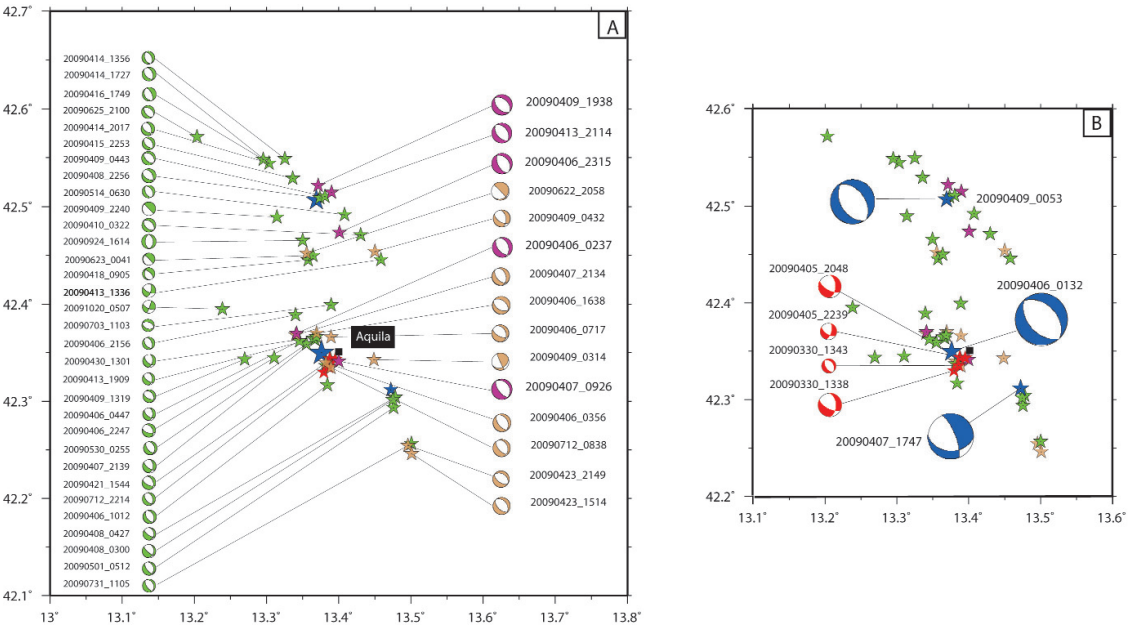


Fig. 11 - Location (this study) and focal mechanisms solution (Scognamiglio *et al*., 2010) of the $M_W$>3.5 events (see also Table 2).

surface where field geologists recognised co-seismic breakages for a length of about 5 km (EMERGEO Working Group, 2010). The location of these ruptures located along the SDP fault agrees with the seismicity termination towards the surface (sections 4, 5 and 6), the splitting of the main fault plane towards the end of the mapped SDP fault marks where it encounters the Mt. Stabiata fault (MS). This segment forms a right lateral step with the SDP located more to the east (see fault traces in Fig. 9). Here the shallower seismicity seems to flatten towards its intersection with the topography. Boncio *et al*. (2010) observed a minor signature of surface ruptures also along ~3 km of the Stabiata fault and their interpretation is that a small amount of slip approached the surface co-seismically. Towards the surface seismicity images minor synthetic splays while in the deepest portions we observed quite large anti- and synthetic faults. Seismicity deeper than 10 km is present also in this area with a small sequence following an $M_W$ 4.2 event that occurred on April 9 (03:14 UTC) that delineates a high angle plane antithetic to the main fault and practically located in its footwall (section 4). The kinematics of this earthquake illustrated by the focal mechanism is very similar with the one shown by the deepest mainshock located in the southern area and described in the previous paragraph.

In sections 7 and 8, we observe many sub-parallel normal faults. In the main fault footwall, we see the southern tip of the Campotosto fault (CMP), located to the east. This means that the Campotosto fault forms an *en-echelon* structure overlapped for almost 6 km, by the MS and SDP system. In between these two systems, we note the presence of another minor sub-parallel segment. The activation of many structures in the main fault footwall is a characteristic of the L'Aquila 2009 system that we did not observe in the 1997 Colfiorito normal fault system

Table 2 - Location (this study), focal mechanisms and source parameters (Scognamiglio *et al*., 2010) for the events with $M_W$>3.5. Grey shaded cells are related to the foreshocks. Earthquakes are ordered by decreasing magnitude.

| DATE | HH.MM | Lat. N(°) | Lon. E(°) | Depth | $M_W$ | Strike 1 | Dip 1 | Rake 1 | Strike 2 | Dip 2 | Rake 2 | Moment |
|---|---|---|---|---|---|---|---|---|---|---|---|---|
| 20090330 | 13:38 | 42.3300 | 13.3795 | 9.2 | 4.0 | 117 | 62 | -129 | 357 | 47 | -40 | 1.06E+22 |
| 20090330 | 13:43 | 42.3353 | 13.3862 | 11.6 | 3.5 | 149 | 53 | -86 | 323 | 37 | -95 | 1.90E+21 |
| 20090405 | 20:48 | 42.3438 | 13.3875 | 9.9 | 3.9 | 119 | 62 | -131 | 0 | 48 | -40 | 8.15E+21 |
| 20090405 | 22:39 | 42.3432 | 13.3952 | 9.6 | 3.5 | 15 | 61 | -35 | 124 | 60 | -145 | 2.21E+21 |
| 20090406 | 1:32 | 42.3502 | 13.3762 | 9.3 | 6.1 | 139 | 48 | -87 | 314 | 42 | -94 | 1.62E+25 |
| 20090407 | 17:47 | 42.3120 | 13.4720 | 14.1 | 5.4 | 338 | 73 | -58 | 93 | 36 | -151 | 1.42E+24 |
| 20090409 | 0:53 | 42.5070 | 13.3687 | 10.9 | 5.2 | 322 | 46 | -95 | 149 | 45 | -85 | 8.25E+23 |
| 20090406 | 23:15 | 42.4735 | 13.4008 | 9.2 | 5.0 | 154 | 57 | -80 | 316 | 34 | -106 | 3.69E+23 |
| 20090409 | 19:38 | 42.5217 | 13.3715 | 7.2 | 5.0 | 137 | 48 | -86 | 311 | 42 | -95 | 3.46E+23 |
| 20090407 | 9:26 | 42.3412 | 13.4000 | 7.5 | 4.9 | 143 | 63 | -91 | 326 | 27 | -88 | 3.06E+23 |
| 20090406 | 2:37 | 42.3700 | 13.3415 | 9.0 | 4.9 | 140 | 53 | -103 | 340 | 39 | -74 | 2.34E+24 |
| 20090413 | 21:14 | 42.5145 | 13.3900 | 7.7 | 4.8 | 138 | 49 | -96 | 327 | 42 | -83 | 2.20E+23 |
| 20090622 | 20:58 | 42.4520 | 13.3557 | 11.1 | 4.4 | 316 | 88 | -76 | 55 | 14 | -170 | 4.36E+22 |
| 20090406 | 3:56 | 42.3397 | 13.3820 | 8.0 | 4.3 | 143 | 55 | -94 | 330 | 35 | -84 | 3.35E+22 |
| 20090407 | 21:34 | 42.3700 | 13.3693 | 7.0 | 4.3 | 310 | 46 | -83 | 120 | 44 | -97 | 3.35E+22 |
| 20090406 | 16:38 | 42.3683 | 13.3402 | 9.0 | 4.3 | 138 | 51 | -106 | 342 | 42 | -72 | 2.92E+22 |
| 20090409 | 3:14 | 42.3428 | 13.4487 | 14.3 | 4.2 | 156 | 87 | 60 | 62 | 30 | 175 | 2.48E+22 |
| 20090712 | 8:38 | 42.3348 | 13.3895 | 9.2 | 4.2 | 138 | 61 | -101 | 341 | 31 | -71 | 2.17E+22 |
| 20090423 | 21:49 | 42.2460 | 13.5013 | 6.5 | 4.2 | 133 | 53 | -96 | 322 | 38 | -82 | 2.30E+22 |
| 20090409 | 4:32 | 42.4537 | 13.4502 | 7.0 | 4.1 | 122 | 54 | -124 | 351 | 48 | -52 | 1.81E+22 |
| 20090406 | 7:17 | 42.3662 | 13.3893 | 7.9 | 4.1 | 118 | 59 | -108 | 329 | 36 | -64 | 1.60E+22 |
| 20090423 | 15:14 | 42.2545 | 13.4960 | 6.4 | 4.0 | 126 | 56 | -88 | 302 | 34 | -93 | 1.19E+22 |
| 20090731 | 11:05 | 42.2565 | 13.5007 | 6.1 | 3.9 | 145 | 60 | -94 | 333 | 30 | -83 | 8.23E+21 |
| 20090924 | 16:14 | 42.4652 | 13.3500 | 13.2 | 3.9 | 178 | 49 | -91 | 359 | 41 | -89 | 9.29E+21 |
| 20090406 | 4:47 | 42.3623 | 13.3455 | 6.3 | 3.8 | 129 | 59 | -123 | 1 | 44 | -48 | 6.70E+21 |
| 20090408 | 4:27 | 42.3042 | 13.4782 | 6.4 | 3.8 | 124 | 71 | -113 | 355 | 29 | -43 | 6.26E+21 |
| 20090408 | 22:56 | 42.5090 | 13.3735 | 8.0 | 3.8 | 329 | 47 | -67 | 117 | 47 | -113 | 7.30E+21 |
| 20090409 | 13:19 | 42.3435 | 13.2695 | 9.8 | 3.8 | 115 | 56 | -108 | 325 | 38 | -66 | 6.30E+21 |
| 20090414 | 13:56 | 42.5490 | 13.3253 | 8.4 | 3.8 | 332 | 46 | -95 | 160 | 45 | -85 | 6.21E+21 |
| 20090415 | 22:53 | 42.5290 | 13.3360 | 8.9 | 3.8 | 132 | 49 | -100 | 328 | 42 | -78 | 6.91E+21 |
| 20090414 | 20:17 | 42.5445 | 13.3035 | 8.6 | 3.7 | 137 | 47 | -107 | 341 | 45 | -72 | 5.07E+21 |
| 20090406 | 21:56 | 42.3888 | 13.3400 | 6.9 | 3.7 | 140 | 46 | -104 | 340 | 46 | -76 | 4.06E+21 |
| 20090409 | 4:43 | 42.5103 | 13.3807 | 8.0 | 3.7 | 136 | 55 | -86 | 308 | 35 | -96 | 4.03E+21 |
| 20090410 | 3:22 | 42.4710 | 13.4302 | 7.3 | 3.7 | 134 | 47 | -88 | 311 | 43 | -92 | 4.11E+21 |
| 20090413 | 19:09 | 42.3645 | 13.3645 | 9.0 | 3.7 | 126 | 63 | -122 | 0 | 41 | -44 | 4.09E+21 |
| 20090416 | 17:49 | 42.5483 | 13.2950 | 9.1 | 3.7 | 335 | 60 | -87 | 150 | 30 | -95 | 4.80E+21 |
| 20090418 | 9:05 | 42.4452 | 13.3577 | 11.5 | 3.7 | 311 | 66 | -110 | 172 | 31 | -53 | 5.17E+21 |
| 20090623 | 0:41 | 42.4498 | 13.3642 | 10.9 | 3.7 | 315 | 85 | -101 | 201 | 12 | -24 | 4.47E+21 |
| 20090703 | 11:03 | 42.3990 | 13.3892 | 4.8 | 3.7 | 289 | 46 | -91 | 111 | 44 | -88 | 5.09E+21 |
| 20090712 | 22:14 | 42.3432 | 13.3882 | 9.1 | 3.7 | 116 | 60 | -115 | 339 | 39 | -54 | 3.73E+21 |
| 20090406 | 10:12 | 42.3170 | 13.3840 | 9.0 | 3.6 | 144 | 51 | -100 | 339 | 40 | -78 | 3.43E+21 |
| 20090406 | 22:47 | 42.3448 | 13.3102 | 10.5 | 3.6 | 104 | 58 | -120 | 332 | 42 | -51 | 3.39E+21 |
| 20090407 | 21:39 | 42.3637 | 13.3670 | 8.5 | 3.6 | 127 | 64 | -123 | 3 | 41 | -42 | 3.29E+21 |
| 20090408 | 3:00 | 42.3018 | 13.4747 | 6.1 | 3.6 | 131 | 73 | -115 | 8 | 30 | -36 | 3.47E+21 |
| 20090409 | 22:40 | 42.4892 | 13.3140 | 11.0 | 3.6 | 316 | 90 | -92 | 220 | 2 | -6 | 3.31E+21 |
| 20090413 | 13:36 | 42.4458 | 13.4583 | 7.4 | 3.6 | 116 | 69 | -152 | 15 | 64 | -24 | 2.94E+21 |
| 20090414 | 17:27 | 42.5445 | 13.3035 | 8.6 | 3.6 | 123 | 50 | -118 | 343 | 47 | -61 | 3.45E+21 |
| 20090501 | 5:12 | 42.2937 | 13.4758 | 6.8 | 3.6 | 142 | 61 | -103 | 347 | 32 | -68 | 2.98E+21 |
| 20090530 | 2:55 | 42.3590 | 13.3553 | 9.6 | 3.6 | 139 | 56 | -106 | 345 | 37 | -68 | 2.73E+21 |
| 20090421 | 15:44 | 42.3367 | 13.3818 | 9.6 | 3.5 | 139 | 54 | -107 | 347 | 40 | -68 | 2.02E+21 |
| 20090430 | 13:01 | 42.3665 | 13.3688 | 8.6 | 3.5 | 131 | 60 | -128 | 8 | 47 | -44 | 2.31E+21 |
| 20090625 | 21:00 | 42.5715 | 13.2037 | 8.0 | 3.5 | 143 | 52 | -76 | 301 | 40 | -107 | 2.07E+21 |
| 20091020 | 5:07 | 42.3948 | 13.2385 | 9.8 | 3.5 | 20 | 81 | -23 | 114 | 67 | -171 | 2.17E+21 |
| 20090514 | 6:30 | 42.4917 | 13.4077 | 7.6 | 3.4 | 154 | 48 | -86 | 328 | 42 | -94 | 1.77E+21 |

(Chiaraluce *et al*., 2003).

Foreshock activity is confined in this area and this is the reason why we draw additional thinner cross sections. Looking at the foreshock sequence in the map view of Fig. 9 (red points), we observe a NW-trending elongated seismicity distribution, consistent with the L'Aquila fault plane related seismicity, and, to the south, an almost N-S branch. Valoroso *et al*. (2009), observed that the sparser seismicity occurred before the foreshock generally nucleated around the main fault plane, whereas after the $M_W$ 4.0 occurred on April 30 at 13:38 UTC (larger red star in section 5 of Fig. 10), seismicity started to activate a minor segment almost antithetic to the main fault plane. Accordingly, the focal mechanism of the $M_W$ 4.0 event shows a high angle E-dipping plane striking N-S with a left lateral component. Then, on April 5, seismicity nucleation moved back to the main fault plane with the occurrence of two events felt by the population (20:48 UTC $M_W$ 3.9 and 22:39 UTC with $M_W$ 3.5; red stars in section 20).

### *4.3. Campotosto area*

The SW-dipping Campotosto fault (sections 9 to 12) shows some notable differences with respect to the MS-SDP one. The fault plane is about 12-14 km long, somewhat smaller than the MS-SDP. In addition, the dip of the fault changes with depth. We discriminate the portion between 8 and 11 km of depth that dips about 35° from the shallower termination that dips steeper (about ~50°) up to a 6 km depth. On the contrary, the deepest part of this complex fault segment shows a tendency to flattening. Focal mechanism solutions are in agreement with these changing in dip. Moreover, the higher magnitude events ($M_W$>4.5) nucleate exactly where the fault plane changes its dip showing a segmented shape (sections 9 and 10 in Fig. 10). The overall picture defines a striking listric geometry observed for the first time by seismicity distribution.

### *4.4. Cittareale area*

A small event with $M_W$ 3.5, occurred on June 25 at 21:00 UTC (green star in section 13 of Fig. 10) which started the occurrence of a cluster of seismicity near the village of Cittareale located at about 8-10 km to the NW of the main fault system. Although this small event is the largest that has occurred in this northernmost area, we observed a clear acceleration in the seismic release soon after its occurrence (Fig. 7). Many small events occurred within a couple of months, with the $M_W$ 3.5 event nucleating at the base of this cluster at an 8 km depth, but their spatial distribution does not allow us to identify any fault geometry. Only in the last section, drowned to the north (section 14), can we distinguish a possible alignment of seismicity. Antonioli *et al*. (2009) modelled the seismicity pattern of this sector and their preliminary results suggest that the spatio-temporal distribution of the seismicity is consistent with a pore-fluid pressure diffusion process.

## 5. Discussion and conclusions

We used seismicity distribution of the 2009 L'Aquila sequence to reconstruct the geometry of the activated normal fault system. We image two main fault segments: the San Demetrio-Paganica-Mt. Stabiata main fault and a second structure in the Campotosto area. The system is composed by SW-dipping planes, as previously proposed by geodetic data (Atzori *et al*., 2009;

Walters *at al.,* 2009). The main shock nucleated at the base of the larger SDP-MS segment is located exactly beneath the ancient city of L'Aquila (Chiarabba *et al*., 2009). The main shock position, together with source directivity (Cirella *et al*., 2009; Ellsworth and Chiaraluce, 2009; Pino and Di Luccio, 2009) and site effects, contributed to the damage (Çelebi *et al*., 2010).

The larger SDP-MS segment (~16 km of length) is a SW-dipping almost planar plane cross-cutting at high angle (50° +/-3°) the whole of the upper crust down to a depth of 10 km. On the contrary, the smallest CMP fault (12-14 km of length) activated between 5 and 12 km of depth, shows a smaller dip (about 35°) and a segmented geometry along the fault width with a tendency to flattening towards the deepest portion. The major events (6 with $M_W$>4.5) that nucleated along this structure are located where the fault changes its dip and the focal mechanism solutions are in agreement with this observation.

The dip showed by the shallower seismicity located along the SDP-MS fault seems to be in agreement with the hypothesis of coseismic ruptures reaching the surface during the main slipping episode, as proposed by many authors based on geodetic (Anzidei *et al*., 2009; Atzori *et al*., 2009; Walters *et al*., 2009) and field geology studies (Falcucci *et al*., 2009; Boncio *et al*., 2010; EMERGEO Working Group, 2010). The innovative application of laser scan technology to survey after-slips seems to corroborate the hypothesis of a fault model where a small amount of slip reached the surface (McCaffrey *et al*., 2009).

Conversely, the CMP segment is completely blind and the overall relationship between the mapped geological structure named Monti della Laga fault and the CMP seismological fault [in the sense of Chiaraluce *et al*. (2005)] is not straightforward due to the lack of seismicity in the first 5 km of the crust. Moreover, a further changing in the dip towards the surface would be needed to align the Campotosto seismicity with the geological fault trace at its intersection with the surface. Chiarabba *et al*. (2009) indicated this portion of the fault not interested by seismicity (an area of about 4 km by 10 km) as the possible location for a future moderate event. Antonioli *et al*. (2009) investigated this aspect by analysing static stress transfers and their preliminary results show that the seismicity that occurred on the deepest portion of the plane may have downloaded the (positive) stress in the upper termination of the fault.

Another important distinction between the Campotosto and the L'Aquila region is the presence in the crustal volume of several secondary structures. They are almost absent in the CMP area while they characterise both the L'Aquila fault hanging and footwalls. We ascribe the different pattern of strain release to significant differences in the crustal structure and lithology between the L'Aquila and Campotosto areas. The upper crust in the mainshock area consists of a complex stack of shelf and slope carbonate units (Latium-Abruzzi platform, Triassic-Palaeogene). These deeply fractured units over thrust Mio-Pliocene flysch deposits along the northern (Laga Flysch) and the eastern (Queglia Unit) margins of the Gran Sasso thrust system (Calamita *et al*., 2004). Deep exploration data are not available in the Gran Sasso region, but the CROP11 seismic profile located about 20 km to the south of the epicentral area indicates that the stack of carbonate thrust sheets is up to 8 km thick (Patacca *et al*., 2008). Whilst the Campotosto area, located to the north of the Gran Sasso thrust system, is characterized by NNW-SSE trending fault-propagation folds, involving Triassic-Miocene sedimentary succession of the Umbria-Marche basinal domain (Mazzoli *et al*., 2005). In the hanging wall of the Mt. della Laga fault, two deep exploration wells (UNMIG, 2009) have penetrated a ~2 km thick plastic sequence (Laga Flysch, Cerrogna Marl and

underlying Bisciaro Fm., lower-upper Miocene) overlying the typical carbonatic multilayer and evaporites of the Umbria-Marche stratigraphic sequence (Triassic-Oligocene). Consequently, brittle limestones characterize the mainshock region, whereas thick plastic Miocene sedimentary successions characterize the Umbria-Marche succession in the Campotosto area. Our speculation is that the latter northern volume may account for a larger component of aseismic deformation within the shallower sedimentary successions that together with the more efficient listric geometry, may result in the absence of a pattern of syn- and antithetic secondary faults.

Moderate and large earthquake sequences in the central and northern Apennines (Italy) typically activate NW-striking normal fault systems accommodating the extensional stretching of the belt. These systems are usually composed by adjacent and *en-echelon* segments usually activated in a relatively short time span. The 2009 L'Aquila seismic sequence showing the activation of a normal fault system through main episodes of seismic ruptures delayed hours to days between them is tuned on this general observation. A complex mechanism of multiple failures on adjacent segments is observed both in recent instrumental and historic events (e.g., the 1997 Umbria-Marche sequence and the 1703 Norcia-Cascia earthquakes). For these events the time lapse between major events activating portions of the same system is in the order of hours or months. Fluids in the upper crust are often invoked to be the driving factor for this domino-like behaviour of multiple shocks, as well as for the migration of seismicity along adjacent faults. During the L'Aquila sequence we observe only a minor episode of seismicity migration occurring during the first two days after the main shock, when seismicity moved to the north-western portion of the system from L'Aquila to Campotosto (Fig. 6). However, the rate of seismic release of the whole sequence can be easily modelled as an Omori like decay of the seismicity production giving evidence that the seismicity pattern behaves as a standard mainshock-aftershock seismic sequence (Omori, 1895). We believe that these findings have to be taken into account when interpreting the observed variations in the $V_P/V_S$ with time. Lucente *et al*. (2010) interpreted the variation of the Poisson ratio observed during the foreshock sequence as an example of dilatancy process that contributed to decrease the normal stress on the main fault plane. While Di Luccio *et al*. (2010) proposed that a pore fluid pressure diffusion process may control the whole space-time evolution of aftershocks sequence.

Finally, as observed for the majority of the larger instrumental events occurred in Italy in the past 20 years, surface evidences of the fault dislocation of the L'Aquila earthquake are tiny, making it difficult to interpret. This aspect amplifies our challenge in precisely locating the segments driving the larger deformation episodes of this portion of the Apennines, as testified by the absence of the San Demetrio-Paganica fault in the consensus catalogue of the active faults of the area (Barchi *et al*., 2000). At the same time we believe that the extraordinary data collected for the L'Aquila sequence by multidisciplinary geophysical networks will allow us a better modelling and interpretation of the deformation style of the area for the future improvement of earthquake hazard models.

## REFERENCES


Aldersons F., Di Stefano R., Chiaraluce L., Piccinini D. and Valoroso L.; 2009: A*utomatic detection and P- and S-wave picking algorithm: an application to the 2009 L'Aquila (Central Italy) earthquake sequence.* In: American Geophys. Union, Fall Meeting 2009, San Francisco December 14-18, < http://adsabs.harvard.edu/abs/2009AGUFM.U23B0045A>.

Antonioli A., Atzori S., Chiarabba C., Chiaraluce L. and Cocco M.; 2009: *Stress evolution during the April 2009 L'Aquila sequence (central Italy).* In: American Geophys. Union, Fall Meeting 2009, San Francisco December 14-18, < http://adsabs.harvard.edu/abs/2009AGUFM.U23B0043A>.

Anzidei M., Boschi E., Cannelli V., Devoti R., Esposito A., Galvani A., Melini D., Pietrantonio G., Riguzzi F., Sepe V. and Serpelloni E.; 2009: *Coseismic deformation of the destructive April 6, 2009 L'Aquila earthquake (central Italy) from GPS data.* Geophys. Res. Lett., **36**, L17307, doi: 10.1029/2009GL039145.

Atzori S., Hunstad I., Chini M., Salvi S., Tolomei C., Bignami C., Stramondo S., Trasatti E., Antonioli A. and Boschi E.; 2009: *Finite fault inversion of DInSAR coseismic displacement of the 2009 L'Aquila earthquake (central Italy).* Geophys. Res. Lett., **36**, L15305, doi: 10.1029/2009GL039293.

Bagh S., Chiaraluce L., De Gori P., Moretti M., Govoni A., Chiarabba C., Di Bartolomeo P. and Romanelli M.; 2007: *Background seismicity in the central Apennines of Italy: the Abruzzo region case study.* Tectonophysics, **444**, 80-92.

Bagnaia R., D'Epifanio A. and Labini S.S.; 1992: *Aquila and subaequan basins: an example of Quaternary evolution in central Apennines, Italy*. Quat. Nova, **2**, 187- 209.

Barchi M., Galadini F., Lavecchia G., Messina P., Michetti A.M., Peruzza L., Pizzi A., Tondi E. and Vittori E. (eds); 2000: *Sintesi delle conoscenze sulle faglie attive in Italia centrale: parametrizzazione ai fini della caratterizzazione della pericolosità sismica.* CNR-Gruppo Naz. per la Difesa dai Terremoti., Roma, 62 pp.

Boncio P., Lavecchia G. and Pace B.; 2004: *Defining a model of 3D seismogenic sources for seismic hazard assessment applications: the case of central Apennines (Italy).* J. Seismol., **8**, 407-425, doi: 10.1023/B:JOSE.0000038449.78801.05.

Boncio P., Pizzi A., Brozzetti F., Pomposo G., Lavecchia G., Di Naccio D. and Ferrarini F.; 2010: *Coseismic ground deformation of the 6 April 2009 L'Aquila earthquake (central Italy, $M_w$6.3).* Geophys. Res. Lett., **37**, L06308, doi:10.1029/2010GL042807.

Calamita F., Viandante M.G. and Hegarty K.; 2004: *Pliocene-Quaternary burial/exhumation paths of the central Apennines (Italy): implications for the definition of the deep structure of the belt.* Boll. Soc. Geol. Ital., **123,** 503-512.

Cavinato G.P. and De Cellis P.G.; 1999: *Extensional basins in the tectonically bimodal central Apennines fold-thrust belt, Italy: response to corner flow above a subduction slab in retrograde motion.* Geology, **27**, 955-958.

Çelebi M., Bazzurro P., Chiaraluce L., Clemente P., Decanini L., DeSortis A., Ellsworth W., Gorini A., Kalkan E., Marcucci S., Milana G., Mollaioli F., Olivieri M., Paolucci R., Rinaldis D., Rovelli A., Sabetta F. and Stephens C.; 2010: *Recorded motions of the $M_w$ 6.3 April 6, 2009 L'Aquila (Italy) earthquake and implications for building structural damage: overview*. Earthquake Spectra, **26**, 651-684.

Chiarabba C., Amato A., Anselmi M., Baccheschi P., Bianchi I., Cattaneo M., Cecere G., Chiaraluce L., Ciaccio M.G., De Gori P., De Luca G., Di Bona M., Di Stefano R., Faenza L., Govoni A., Improta L., Lucente F.P., Marchetti A., Margheriti L., Mele F., Michelini A., Monachesi G., Moretti M., Pastori M., Piana Agostinetti N., Piccinini D., Roselli P., Seccia D. and Valoroso L.; 2009: *The 2009 L'Aquila (central Italy) $M_W$6.3 earthquake: main shock and aftershocks.* Geophys. Res. Lett., **36,** L18308, doi: 10.1029/2009GL039627.

Chiaraluce L., Barchi M., Collettini C., Mirabella F. and Pucci S.; 2005: *Connecting seismically active normal faults with Quaternary geological structures in a complex extensional environment: The Colfiorito 1997 case history (northern Apennines, Italy).* Tectonics, **24**, TC1002, doi: 10.1029/2004TC001627.

Chiaraluce L., Chiarabba C., Collettini C., Piccinini D. and Cocco M.; 2007: *Architecture and mechanics of an active low-angle normal fault: Alto Tiberina Fault, northern Apennines, Italy.* Jour. Geophys. Res., **112**, B10310, doi: 10.1029/2007JB005015.

Chiaraluce L., Ellsworth W.L., Chiarabba C. and Cocco, M.; 2003: *Imaging the complexity of an active normal fault system: the 1997 Colfiorito (central Italy) case study.* Jour. Geophys. Res. **108**, 2294-2313. doi: 10.1029/2002JB002166.

Chiaraluce L., Valoroso L., Anselmi M., Bagh S. and Chiarabba C.; 2009: *A decade of passive seismic monitoring experiments with local networks in four Italian regions.* Tectonophysics, **476**, 85-98.

Ciaccio M.G., Palombo B. and Bernardi F.; 2009: *The main seismic sequences occurred between 1981-2008 in the L'Aquila region*. In: Proceedings FIST, Rimini 9-11 September 2009.

Cirella C., Piatanesi A., Cocco M., Tinti E., Scognamiglio L., Michelini A., Lomax A. and Boschi E.; 2009: *Rupture history of the 2009 L'Aquila (Italy) earthquake from non-linear joint inversion of strong motion and GPS data.* Geophys. Res. Lett., **36**, L19304, doi: 10.1029/2009GL039795.

CPTI Working Group; 1999: *Catalogo parametrico dei terremoti italiani*. ING, GNDT, SGA, SSN, Bologna, 92 pp, < http://emidius.mi.ingv.it/CPTI/>.

D'Agostino N., Giuliani R., Mattone M. and Bonci L.; 2001: *Active crustal extension in the central Apennines (Italy) inferred from GPS measurements in the interval 1994-1999.* Geophys. Res. Lett., **28**, 2121-2124.

De Luca G., Scarpa R., Filippi L., Gorini A., Marcucci S., Marsan P., Milana G. and Zambonelli E.; 2000: *A detailed analysis of two seismic sequences in Abruzzo, central Apennines, Italy*. Jour. Seismol., **4**, 1-21.

Deschamps A., Iannaccone G. and Scarpa R.; 1984: *The Umbrian earthquake (Italy) of 19 September 1979*. Annales Geophysicae, **2**, 29-36.

Di Luccio F., Ventura G., Di Giovambattista R., Piscini A. and Cinti F.R.; 2010: *Normal faults and thrusts reactivated by deep fluids: The 6 April 2009 $M_w$ 6.3 L'Aquila earthquake, central Italy*. Jour. Geophys. Res., 115, B06315, doi: 10.1029/2009JB007190.

Di Stefano R., Chiarabba C., Chiaraluce L., Cocco M., De Gori P., Piccinini D. and Valoroso L.; 2011: *Fault properties heterogeneity affecting the rupture evolution of the 2009 ($M_w$ 6.1) L'Aquila earthquake (Central Italy): insights from seismic tomography.* Geophys. Res. Lett., submitted.

Ellsworth W. and Chiaraluce L.; 2009: *Supershear during nucleation of the 2009 M 6.3 L'Aquila, Italy earthquake*. In: American Geophys. Union. Fall Meeting 2009, San Francisco December 14-18, <http://adsabs.harvard.edu/abs/2009AGUFM.U13C.07E>.

EMERGEO Working Group; 2010: *Evidence for surface rupture associated with the $M_w$ 6.3 L'Aquila earthquake sequence of April 2009 (central Italy)*. Terra Nova, **22**, 43-51, doi: 10.1111/j.1365-3121.2009.00915.x.

Falcucci E., Gori S., Peronace E., Fubelli G., Moro M., Saroli M., Ciaccio B., Messina P., Naso G., Scardia G., Sposato A., Voltaggio M., Galli P. and Galadini F.; 2009: *The Paganica fault and surface coseismic ruptures caused by the 6 April 2009 earthquake (L'Aquila, central Italy).* Seismol. Res. Lett., **80**, 940-950, doi: 10.1785/gssrl.80.6.940.

Galadini F. and Galli P.; 2000: *Active tectonics in the central Apennines (Italy)-input data for seismic hazard assessment.* Nat. Hazards, **22**, 225-270.

Galadini F. and Galli P.; 2003: *Paleoseismology of silent faults in the central Apennines (Italy): the Mt. Vettore and Laga Mts. faults.* Ann. Geophys., **5**, 815-836.

Hunstad I., Selvaggi G., D'Agostino N., Englaand P., Clarke P. and Pierozzi M.; 2003: *Geodetic strain in peninsular Italy between 1875 and 2001.* Geophys. Res. Lett., **30**, 1181-1185.

Kissling E., Ellsworth W.L., Eberhart-Phillips D. and Kradolfer U.; 1994: *Initial reference models in local earthquake tomography.* Jour. Geophys. Res., **99**, 19635-19646.

Lahr J.C.; 1989: *HYPOELLIPSE/version 2.00: a computer program for determining local earthquakes hypocentral parameters, magnitude and first motion pattern*. U.S. Geol. Surv. Open-File Rep., 89-116, 92 pp.

Lavecchia G., Brozzetti F., Barchi M., Keller J. and Menichetti M.; 1994: *Seismotectonic zoning in east-central Italy deduced from the analysis of the Neogene to present deformations and related stress fields*. Geol. Soc. Am. Bull., **106**, 1107-1120.

Lucente F.P., De Gori P., Margheriti L., Piccinini D., Di Bona M., Chiarabba C. and Agostinetti N. P.; 2010: *Temporal variation of seismic velocity and anisotropy before the 2009 $M_W$ 6.3 L'Aquila earthquake, Italy.* Geology, **38**, 1015-1018, doi: 10.1130/G31463.1.

Mariucci M.T., Amato A. and Montone, P.; 1999: *Recent tectonic evolution and present day stress in the northern Apennines (Italy)*. Tectonics, **18**, 108-118.

Mazzoli S., Pierantoni P.P., Borraccini F., Paltrinieri W. and Deiana G.; 2005: *Geometry, segmentation pattern and displacement variations along a major Apennine thrust zone, central Italy*. Jour. Structural Geology, **27**, 1940-1953.

McCaffrey K.J., Wilkinson M., Roberts G., Cowie P.A., Phillips R., Walters R.J., Barba S., La Rocca L., Vittori E., Blumetti A., Guerrieri L., Guzzetti F., Lollino G., Porfido S., Esposito E., Piccardi L., Campedel P., Cocco S., Sileo G. and Michetti A.M.; 2009: *Post-seismic slip on the 6th April 2009 L'Aquila earthquake surface rupture, measured using a terrestrial laser scanner (tripod?mounted lidar).* In: American Geophysical Union, Fall Meeting 2009,

<http://adsabs.harvard.edu/abs/2009AGUFM.U23A0023M>.

Montone P., Mariucci M.T., Pondrelli S. and Amato A.; 2004: *An improved stress map for Italy and surrounding regions (central Mediterranean).* Jour. Geophys. Res., **109**, B10410, doi: 10.1029/ 2003JB002703.

Omori F.; 1895: *On the aftershocks of earthquakes.* Jour. College Sci. Imper. Univ. Tokyo, **7**, 111-200.

Pace B., Boncio P. and Lavecchia G.; 2002: *The 1984 Abruzzo earthquake (Italy): an example of seismogenic process controlled by interaction between differently oriented synkinematic faults.* Tectonophysics, **350**, 237-254.

Patacca E., Scandone P., Di Luzio E., Cabinato G.P. and Parlotto M.; 2008: *Structural architecture of the central Apennines: interpretation of the CROP11 seismic profile from the Adriatic coast to the orographic divide.* Tectonics, **27**, TC3006.

Pino N.A. and Di Luccio F.; 2009: S*ource complexity of the 6 April 2009 L'Aquila (central Italy) earthquake and its strongest aftershock revealed by elementary seismological analysis.* Geophys. Res. Lett., **36**, L23305, doi: 10.1029/2009GL041331.

Roberts G.P. and Michetti A.; 2004: *Spatial and temporal variations in growth rates along active normal fault systems; an example from the Lazzio-Abruzzo Apennines, central Italy.* Jour. Struct. Geol., **26**, 339-376.

Scognamiglio L., Tinti E., Michelini A., Dreger D.S., Cirella A., Cocco M., Mazza S. and Piatanesi A.; 2010: *Fast determination of moment tensors and rupture history: what has been learned from the 6 April 2009 L'Aquila earthquake sequence.* Seism. Research Lett., **81**, 892-906, doi: 10.1785/gssrl.81.6.892.

Selvaggi G., Castello B. and Azzara A.; 1997: *Spatial distribution of scalar seismic moment release in Italy (1983-1996): seismotectonic implications for the Apennines.* Ann. Geofis., **40**, 1565-1578.

UNMIG (Italian National Mine Office); 2009: Wells Database available on website: http://unmig.sviluppoeconomico.gov.it/unmig/pozzi/pozzi.asp.

Valoroso L., Amato A., Cattaneo M., Cecere G., Chiarabba C., Chiaraluce L., de Gori P., Delladio A., De Luca G., Di Bona M., Di Stefano R., Govoni A., Lucente F.P., Margheriti L., Mazza S., Monachesi G., Moretti M., Olivieri M., Piana Agostinetti N., Selvaggi G., Improta L., Piccinini D., Mariscal A., Pequegnat C., Schlagenhauf A., Salaun G., Traversa P., Voisin C., Zuccarello L. and Azzaro R.; 2009: *The 2009 L'Aquila seismic sequence (central Apennines): fault system geometry and kinematics.* In: American Geophys. Union, Fall Meeting 2009, San Francisco December 14-18, < http://adsabs.harvard.edu/abs/2009AGUFM.U12A..04V>.

Vezzani L. and Ghisetti F.; 1998: *Carta geologica dell'Abruzzo, scala 1:100000.* S.EL.CA, Firenze.

Walters R.J., Elliott J.R., D'Agostino N., England P.C., Hunstad I., Jackson J.A., Parsons B., Phillips R.J. and Roberts G.; 2009: *The 2009 L'Aquila earthquake (central Italy): a source mechanism and implications for seismic hazard.* Geophys. Res. Lett., **36**, L17312, doi: 10.1029/2009GL039337.

Ward S.N. and Valensise G.R.; 1989: *Fault parameters and slip distribution of the 1915 Avezzano, Italy, earthquake derived from geodetic observations.* Bull. Seismol. Soc. Am., **79**, 690-710.

*Corresponding author:* Raffaele Di Stefano
Ist. Nazionale di Geofisica e Vulcanologia
Via di Vigna Murata 605, 00143 Roma, Italy
Phone: +39 06 51860306; fax: +36 06 51860541; e-mail: raffaele.distefano@ingv.it